TEXTURAL AND STRUCTURAL PROPERTIES OF BIOACTIVE GLASSES IN THE SYSTEM $CaO–SiO_2$

NICHOLA J. COLEMAN, MARIA BELLANTONE*, JOHN W. NICHOLSON, ANDREW P. MENDHAM

School of Science, University of Greenwich, Chatham Maritime, Kent, ME4 4TB, UK
**Nature Materials, The Macmillan Building, 4 Crinan Street, London, N1 9XY, UK*

E-mail: nj_coleman@yahoo.co.uk

Submitted July 17, 2006 ; accepted November 8, 2006

Keywords: Sol-gel, Bioactive, Mesoporous, Glass

Gel-derived CaO-SiO_2 binary glasses of CaO mole fractions 0.2, 0.3 and 0.4 have been prepared and characterised. Pore diameter, specific pore volume, skeletal density and porosity were found to increase with increasing CaO-content, whereas a concomitant decrease in specific surface area was observed. ^{29}Si NMR indicated that the 0.2 CaO mole fraction glass consisted of highly polymerized Q^4 and Q^3 silicate species, with some Q^2 units. With increasing CaO mole fraction, these silicate species became progressively depolymerised such that isolated SiO_4 tetrahedra were detected within the 0.4 CaO glass matrix. Unusually, the glasses retained a proportion of Q^4 and Q^3 species as the CaO mole fraction was increased. All glass formulations exhibited in vitro bioactivity. The rate of hydroxyapatite precipitation followed the order 0.2 CaO > 0.4 CaO > > 0.3 CaO, an effect that is attributed to differences in the rate of dissolution of calcium from these glasses. This, in turn, appears to be dependent upon the proportion of Ca^{2+} participating in the formation of the glassy network.

INTRODUCTION

Commonly, the body's defence mechanism will stimulate the formation of a fibrous capsule around a foreign implant material in an attempt to isolate it from the host tissue; however bioactive materials elicit a specific response from living tissues in which a chemical bond is established at the implant-tissue interface [1,2]. Natural calcite [3] and β-tricalcium phosphate [4] are uniquely capable of forming a direct bond to living bone tissue although all other bioactive materials bond to bone *via* a layer of substituted hydroxyapatite (HA) which precipitates spontaneously at the surface on implantation. This HA-layer provides a focus for the attachment and proliferation of bone-forming cells (osteoblasts) and stimulates bone regeneration *in situ*.

Human body fluid is supersaturated with respect to hydroxyapatite, the calcium phosphate phase which constitutes the inorganic component of bone tissue. Bioactive materials comprise a range of glass and ceramic phases which provide nucleation sites for the precipitation and growth of HA *in vivo* and certain formulations are also designed to release calcium and phosphate ions which increase the extent of supersaturation and enhance the kinetics of the bone-bonding process. The bone-bonding capability of a candidate bioactive material is initially evaluated by investigating its ability to effect the formation of an HA-layer from simulated body fluid (SBF) which is an acellular liquor with an ionic composition which approximates to that of human blood plasma. The validity of this method has been demonstrated by the strong correlation between the formation of the apatite layer during *in vitro* SBF exposure and that observed *in vivo* [1].

The bioactivity of non-porous melt-derived glasses is directly dependent upon composition as indicated in the ternary phase diagram for glasses in the system $Na_2O–CaO–SiO_2$–(6wt.% P_2O_5) shown in Figure 1 [5]. Compositions within regions A, B and C are, respectively, bioactive, non-bioactive, and soluble, whereas those in D are non-glass-forming. The bioactivity of porous sol-gel-derived glasses is both a function of composition and textural properties such as surface area, porosity and pore size distribution [6]. By virtue of their textural characteristics and the presence of surface Si–OH groups which act as HA-nucleation sites, gel-derived porous glasses exhibit bioactivity over an extended compositional range with respect to that of melt-derived glasses [6,7]. Even pure sol-gel-derived SiO_2 matrices have been shown to be capable of precipitating apatite layers onto their surfaces on exposure to SBF [8]. Owing to the complicated inter-dependence between parameters such as composition, pore-size, surface area, porosity and density, the relationship between bioactivity, composition and texture is not presently understood. For example, the observation by

Peltola et al. [6], that high mesopore volumes promote apatite nucleation is in conflict with the findings of Vallet-Regí et al. [9] who report that the rate of formation of apatite increases as a function of macroporosity. Similar discrepancies in bioactivities and textural characteristics of gel-derived glasses in the binary system $CaO–SiO_2$ have also been noted [9,10].

The research reported in the current paper was carried out to investigate aspects of the bioactivity, texture and structure of porous sol-gel-derived glasses in the system $CaO–SiO_2$ for which the mole fractions of CaO are 0.2, 0.3 and 0.4. The bioactivities of the glasses were evaluated by response to *in vitro* SBF exposure, their initial textural properties were characterised using nitrogen gas sorption and their silicate structures were investigated by ^{29}Si nuclear magnetic resonance (NMR) spectroscopy. The changes in textural properties of the glass matrices during residence in SBF and the concomitant dissolution profiles of silicon and calcium are also reported.

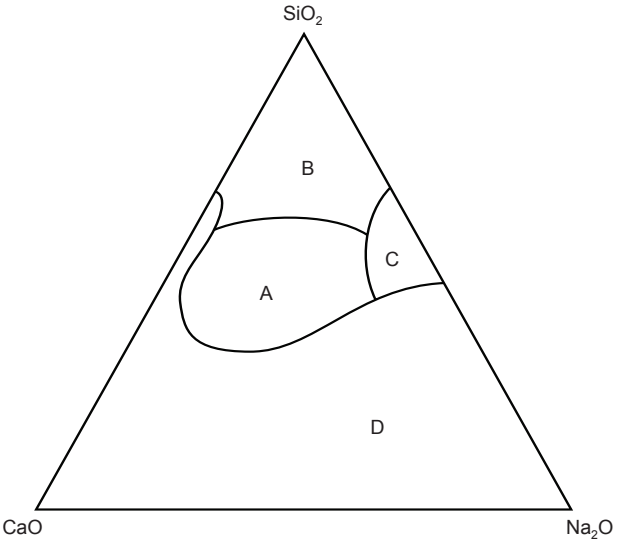

Figure 1. Ternary phase diagram for the glass system Na_2O-CaO-SiO_2-(6wt.% P_2O_5). A - bioactive; B - non-bioactive; C - soluble; D - non-glass-forming.

EXPERIMENTAL

Sol-gel preparation

Two-component glasses were prepared by sequential additions of tetraethoxysilane, $Si(OC_2H_5)_4$, and calcium nitrate tetrahydrate, $Ca(NO_3)_2{\cdot}4H_2O$ to 2N hydrochloric acid at 25°C in the molar proportions listed in Table 1. In each case, $Si(OC_2H_5)_4$ was added to the reaction mixture in small increments under continual stirring, such that the maximum temperature rise was below 10°C, prior to the incremental addition of $Ca(NO_3)_2{\cdot}4H_2O$. The resulting mixture was then stirred for 1 hour, cast into cylindrical screw-capped containers and allowed to gel at 25°C for 72 hours. The resulting gels were then aged at 60°C for a further 72 hours before being dried and stabilised in accordance with the temperature regime depicted in Figure 2. The heating rate between different stages of the drying and stabilisation procedure was 0.1°C/min. Each synthesis was carried out in duplicate and yielded 25 individual gels per batch. The binary gel-derived glasses were stored at room temperature in screw-capped polypropylene containers until required.

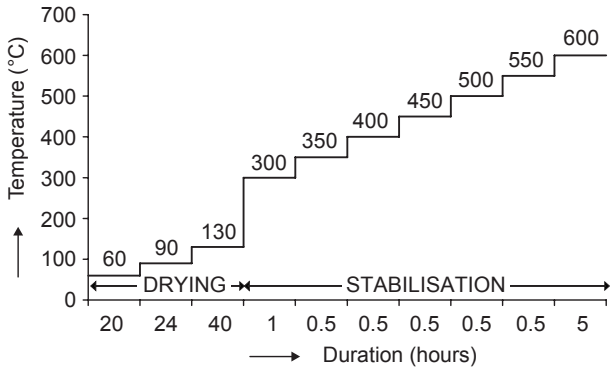

Figure 2. Drying and stabilisation temperatures for binary gel-derived glasses. (It should be noted that the heating rate between each isothermal stage of the drying and stabilisation regime was 0.1°C/min).

Table 1. Compositions of binary gel-derived glasses.

Sample	$Si(OC_2H_5)_4$: $Ca(NO_3)_2{\cdot}4H_2O$: H_2O (molar ratios)	CaO-content (mol%)	SiO_2-content (mol%)
20C:80S	1 : 0.250 : 12	20	80
30C:70S	1 : 0.429 : 12	30	70
40C:60S	1 : 0.667 : 12	40	60

In vitro bioactivity and dissolution characteristics

Simulated body fluid (SBF) was prepared in accordance with the method described in reference 8 and stored in polyethylene bottles at 4°C for no longer than 5 days. The binary glass specimens were immersed in SBF in hermetically-sealed polymethylpentene containers at 37°C for 3, 6, 24, 48, 72 and 168 h. The ratio of geometric surface area to solution volume was fixed at 0.1 cm^{-1}. Each analysis was carried out in quadruplicate. The specimens were recovered, rinsed in acetone and dried in an oven at 60°C for a minimum of 4 h. The development of the HA-layer was monitored using a Midac Series FTIR spectrophotometer to detect diffuse radiation reflected by the surface of the bulk sample. The dissolution of silicon and calcium from the specimens and the removal of phosphorus from SBF during HA-formation were measured using inductively coupled plasma analysis (ICP). The instrument detection limits for Si, Ca and P were 0.05, 0.10 and 0.20 ppm, respectively. The relative standard deviations for all mean values of Si, Ca and P concentration were found to be lower than 5 %.

Materials characterisation

Textural characterisation was carried out by nitrogen gas-sorption using a Quantachrome AS6 Autosorb analyser as described in detail elsewhere [11, 12]. 20 adsorption and 20 desorption isotherm data points were collected and analysed in accordance with ISO 9277:1995(E) 'Determination of the specific surface area of solids by gas adsorption using the BET method'. Five replicates of each sample-type were analysed and two isotherms were collected for each specimen to ensure that the data were representative. Estimates of specific pore volume (V_p) were obtained from the quantity of nitrogen taken up by samples in the range $0.9947 < P/P_0 < 0.9956$ (where P and P_0 are the equilibrium pressure and saturated vapour pressure of nitrogen at 77.4 K, respectively).

The skeletal (true) density was measured by helium pycnometry using a Quantachrome helium Ultrapycnometer 1000. Prior to analysis the samples were degassed at 200°C for 24 h under vacuum to remove physically adsorbed species from their surfaces. The specimens were flushed with helium gas 40 times prior to the collection of data. The skeletal density was taken as the average of 20 measurements.

^{29}Si magic angle spinning (MAS) and ^{1}H-^{29}Si cross-polarisation magic angle spinning (CP-MAS) NMR spectra were recorded at 59.7 MHz using a JEOL JNM-ECP300 FT NMR instrument incorporating an SH30T6/ /HS solid state probe. ^{29}Si spectra were collected using spinning frequencies of approximately 4 kHZ and a relaxation delay of 60 s. Chemical shift values were measured relative to that of tetramethylsilane (TMS).

RESULTS AND DISCUSSION

Characterisation of gel-derived CaO–SiO$_2$ glasses

Following thermal treatment at 600°C, the binary CaO–SiO$_2$ gel-derived glasses prepared during this investigation can be handled routinely without physical disintegration and are sufficiently stable to withstand rehydration stresses when immersed in aqueous media such as simulated body fluid. The initial textural parameters - specific surface area (S_a), mean and modal pore diameter, specific pore volume (V_p), skeletal density (ρ_{sk}) and porosity - of the gel-derived glasses prior to exposure to SBF are listed in Table 2. The values in parentheses are one standard deviation of the mean in each case. The nitrogen gas adsorption-desorption isotherms (not shown) from which the textural parameters are derived are of BDDT type IV indicating that the glasses are mesoporous (i.e. they possess pore diameters in the 20-500 Å range) [13]. Such isotherms are typical of those reported for many gel-derived silica matrices [6,9,11,14]. The isotherms show reproducible H1-type hysteresis in the multilayer region arising from capillary condensation in the mesopore structure which is indicative of the presence of narrowly distributed cylindrical pores [15] and t-Method analysis confirmed the absence of micropores [16].

The textural analysis shows that pore diameter, specific pore volume, skeletal density and porosity increase as functions of mole fraction of CaO, whereas specific surface area decreases with increasing CaO:SiO$_2$ ratio. In each case the modal pore diameter is notably smaller

Table 2. Textural properties of gel-derived CaO–SiO$_2$ glasses.

Sample	S_a (m^2/g)	Mean Dia. (Å)	Modal Dia. (Å)	V_p (cm^3/g)	ρ_{sk} (g/cm^3)	Porosity (%)
20C:80S	138 (± 4)	166 (± 12)	136 (± 24)	0.573 (± 0.036)	2.32 (± 0.07)	57.0
30C:70S	118 (± 3)	230 (± 9)	177 (± 1)	0.679 (± 0.018)	2.46 (± 0.01)	62.5
40C:60S	91 (± 13)	303 (± 37)	235 (± 34)	0.683 (± 0.022)	2.53 (± 0.02)	63.5

S_a - specific surface area; Dia. - pore diameter; V_p - specific pore volume and ρ_{sk} - skeletal density.

than the mean pore diameter. This difference between the two quantities arises from a combination of factors including; deviation from perfect cylindrical geometry, the volume associated with the junctions of the pores and the existence of a small number of large pores [11]. Vallet-Regi et al. [9] prepared binary $CaO–SiO_2$ sol-gels in the compositional range 0.1 < CaO mole fraction < 0.5 which, after drying, were ground and compacted at 150 MPa into discs prior to stabilisation at 700°C. The observed trends in textural properties with respect to $CaO:SiO_2$ ratio for the gel-glasses prepared from the compacted stabilised discs are generally similar to those reported in this study with the exception of specific pore volume and porosity which are reported to decrease from 0.447 to 0.298 cm^3/g and 60.0 to 53.6 %, respectively, as the mole fraction of CaO is increased from 0.2 to 0.4. It should also be noted that the specific pore volumes of the gel-glasses produced *via* grinding and compaction are significantly smaller than those of the monolithic articles acquired directly from the cast gels prepared in this study.

Skeletal density values obtained in this study are within 1% of those reported by Vallet-Regi et al. [9] (2.317-2.550 g/cm^3) and correspond well with the theoretical values expected for glasses in this compositional range [18]. Conversely, other researchers have reported skeletal densities between 1.6 and 1.3 g/cm^3 for binary gel-glasses in this system, although it is likely that these remarkably low values may have arisen from incomplete de-gassing during sample preparation for helium pycnometry [10].

^{29}Si MAS NMR spectra for the binary gel-derived glasses are shown in Figure 3 and the corresponding signal maxima, frequency widths at half maximum peak height (FWHM) and signal ranges are listed in Table 3. The common notation used to describe local silicate environments in glasses and ceramics is such that the symbol Q represents one SiO_4^{4-} tetrahedron and a superscript, n, denotes the number of other Q units to which it is bonded *via* Si–O–Si linkages. For example, a mid-chain SiO_4^{4-} unit linked to two other SiO_4^{4-} units would be represented thus - Q^2.

The ^{29}Si MAS NMR spectrum of 20C:80S (Figure 3a) comprises an asymmetrical compound resonance of maximum intensity at -112.9 ppm arising from Q^4 silicate species with a pronounced low-field shoulder at -100 ppm (Q^3) and a minor contribution centred around -90 ppm (Q^2) [18]. Hence, the silicate network of 20C:80S is predominantly composed of highly polymerised Q^4 and Q^3 species with a small proportion of Q^2 silicate tetrahedra. The chemical shift range for the 20C:80S signal spans from -87 to -123 ppm and the FWHM of 14.5 ppm. Other researchers also report poorly-resolved compound signals and similar FWHM values for melt-derived bioactive glasses in the four-component system $Na_2O–CaO–SiO_2–P_2O_5$ [5]. The broad linewidths arise from a continuous distribution of local structural environments for each of the Q^n species present in the glasses which derive from different O–Si–O bond angles, the proximity and abundance of neighbouring Ca^{2+} and the presence of Si–OH species.

The broad asymmetric resonance in the ^{29}Si MAS NMR spectrum of 30C:70S (Figure 3b) spans the chemical shift range from -75 to -123 ppm and is indicative of a highly disordered silicate network comprising a range of environments from Q^1 to Q^4. A comparison of the ^{29}Si MAS NMR data for samples 20C:80S and 30C:70S shows that an increase in mole fraction of CaO from 0.2 to 0.3 causes considerable depolymerisation and structural disorder within the silicate network. Similarly, an increase in the mole fraction of CaO to 0.4 also

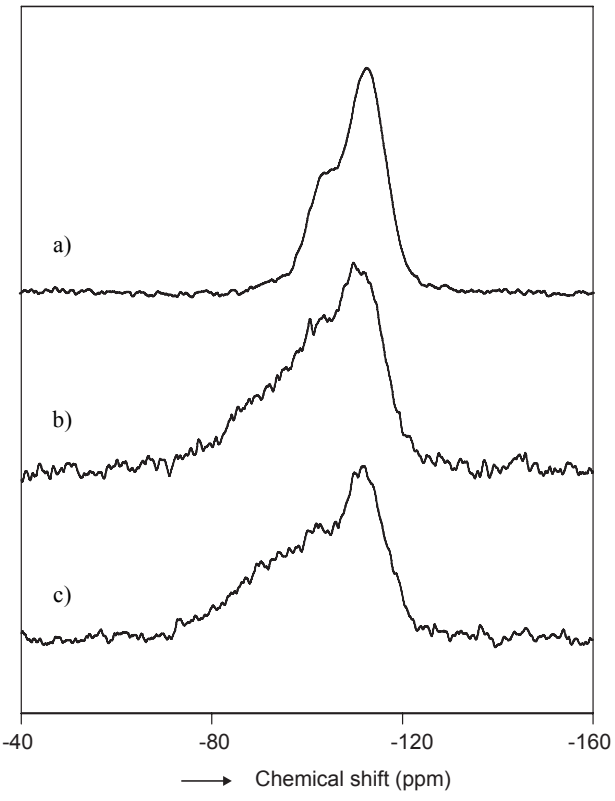

Figure 3. ^{29}Si MAS NMR spectra of: a) 20C:80S, b) 30C:70S and c) 40C:60S.

Table 3. ^{29}Si NMR peak maxima, FWHM and signal ranges for gel-derived $CaO–SiO_2$ glasses.

Sample	Peak maximum (ppm)	FWHM (ppm)	Signal range (ppm)
20C:80S	-112.9	14.5	-87 to -123
30C:70S	-109.9	20.1	-75 to -123
40C:60S	-112.2	22.8	-69 to -123

further increases the extent of depolymerisation and introduces isolated silicate tetrahedra into the glass matrix. This is demonstrated by the extension of the chemical shift range for sample 40C:60S (-69 to -123 ppm) into the Q^0 region (Figure 3c).

An unusual feature of samples 30C:70S and 40C:60S is that their silicate networks are composed of four- and five-site Qn distributions, i.e. ranges including Q^1 to Q^4 and Q^0 to Q^4 silicate species, respectively. It is generally acknowledged that increasing additions of CaO as replacement for SiO_2 in melt-derived glasses bring about the sequential depolymerisation of the glass network [5]. The nature of the depolymerisation in melt-derived glasses is such that two- and three-site Q^n distributions are observed; i.e. glasses contain distributions of Q^4 to Q^2, Q^3 to Q^1 or Q^2 to Q^0 silicate species depending on the proportion of CaO and presence of other network modifiers. It is extremely rare for melt-derived glasses to comprise four- and five-site Q^n distributions such as those observed here for the gel-derived glasses, 30C:70S and 40C:60S. It is, in all probability, this unique retention of Q^4 and Q^3 species at high $CaO:SiO_2$ ratios that extends the compositional range of sol-gel-derived glasses into the non-glass-forming region of the melt-derived system.

The ^1H-^{29}Si CP MAS NMR spectra of the binary gel-derived glasses are presented in Figure 4 and demonstrate the persistence of significant residual

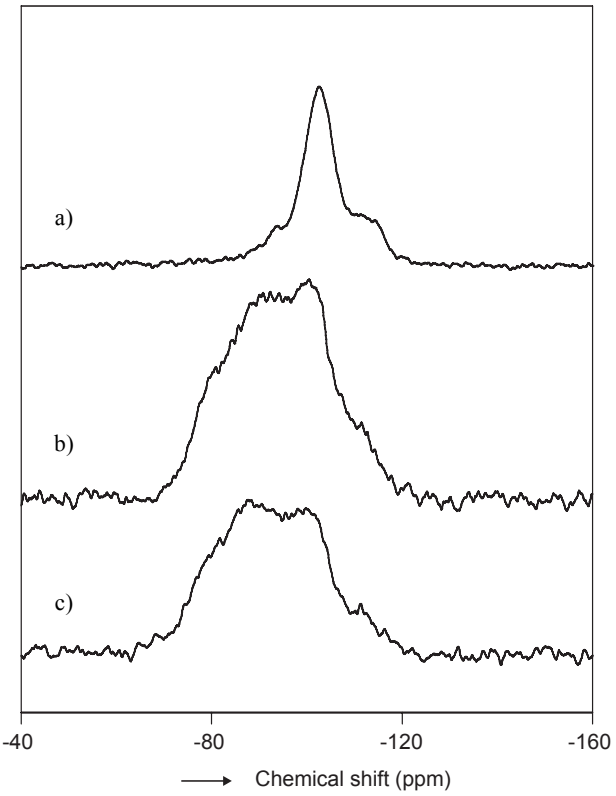

Figure 4. ^1H–^{29}Si CP MAS NMR spectra of: a) 20C:80S, b) 30C:70S and c) 40C:60S.

silanol (Si–OH) groups following stabilisation at 600°C. Chemically-bound water may also be present. As previously mentioned, Si–OH groups are relevant to bioactivity as they provide nucleation sites for the precipitation of hydroxyapatite. It should be noted that the signal intensities recorded in CP spectra are functions of relaxation and contact parameters, number of neighbouring protons and their ^1H-^{29}Si inter-nuclear distances, hence, they are not proportional to the relative abundance of the different Q^n species.

In vitro bioactivity and dissolution characteristics

A semiquantitative measure of bioactivity can be obtained from the rate of formation of a substituted hydroxyapatite layer on the surface of a material *in vitro* in SBF [1]. Accordingly, the kinetics of *in vitro* formation of HA on the surface of samples 20C:80S, 30C:70S

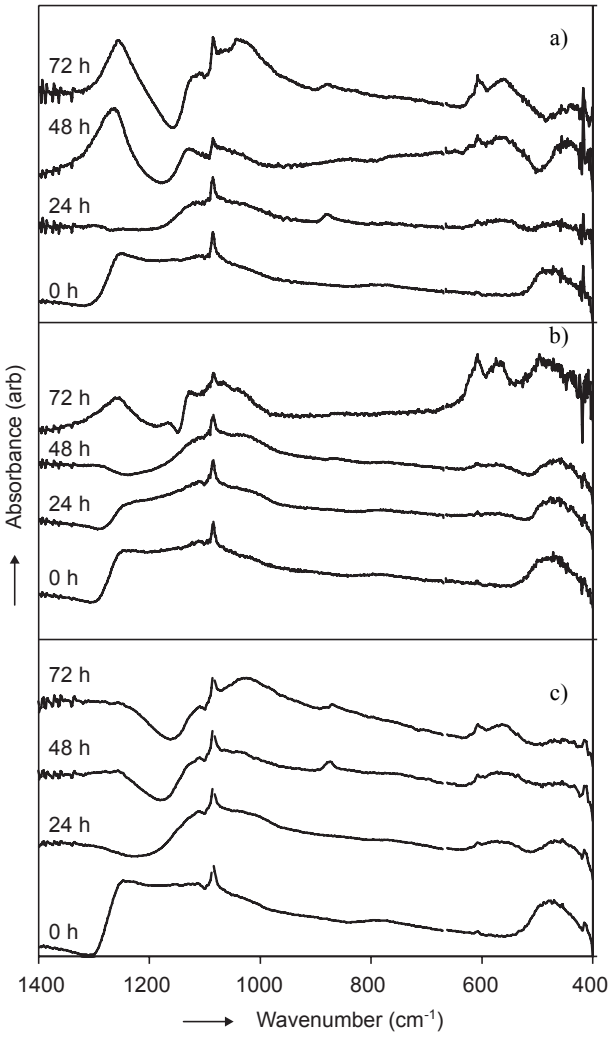

Figure 5. Diffuse reflectance FTIR spectra of the surfaces of a) 20C:80S, b) 30C:70S and c) 40C:60S as functions of exposure to SBF.

and 40C:60S have been monitored using diffuse reflectance FTIR spectroscopy and ICP. FTIR spectra of the surfaces of gel-derived glasses as functions of residence time in SBF are presented in Figure 5 and the corresponding SBF-concentration profiles for Ca, P and Si are also shown in Figure 6. The spectra of the glass samples prior to exposure to SBF comprise broad silicate absorption bands at approximately 480 cm^{-1}, 1100 cm^{-1} and 1200 cm^{-1} which are assigned to Si–O bending, transverse Si–O stretching and longitudinal Si–O stretching, respectively [19]. The broad band of low intensity centred around 580 cm^{-1} in the FTIR spectra of 20C:80S and 40C:60S (Figures 5a and 5c, respectively) following a residence period of 24 hours is evidence of the formation of a layer of amorphous calcium phosphate on the surfaces of the samples. The subsequent development of a layer of crystalline hydroxyapatite is shown by the resolution of this signal into two peaks at 570 and 605 cm^{-1} and the crystallographic substitution of carbonate ions into the apatite structure is denoted by the signal at 870 cm^{-1}. The concomitant removal of phosphate species from SBF in contact with 20C:80S and 40C:60S is shown in Figures 6a and 6c, respectively, and is consistent with the FTIR data. The concentration of phosphate species is seen to decrease markedly between 24 and 48 hours to below 0.1 mM in both cases. The data indicate that the onset of HA-precipitation is similar for both 20C:80S and 40C:60S, although the stronger, better-resolved FTIR phosphate signals after 48 and 72 hours in the former case suggest that the HA-layer on sample 20C:80S possesses superior structural order. In comparison the kinetics of removal of phosphate ions from SBF and the formation of HA on the surface of sample 30C:70S (Figures 6b and 5b, respectively) are relatively slow, although by 72 hours a well-developed apatite layer is seen to have formed.

The results of *in vitro* SBF-analyses have shown that the rates of precipitation of HA on the surfaces of the binary gel-derived glasses are of the following order: 20C:80S > 40C:60S > 30C:70S, although the HA-layer which forms on the surface of 40C:60S is ultimately less crystalline than those of the other glasses. The observed kinetic trend is likely to have arisen from the differences in Ca- and Si-dissolution from the glasses. Increases in calcium ion concentration in solution will enhance the supersaturation of SBF with respect to HA and hence promote precipitation. The results indicate that calcium dissolution is not proportional to the relative mole fractions of CaO in the glasses and that the rate and extent of Ca-dissolution from 30C:70S is inferior to those of 20C:80S and 40C:60S (Figure 6). Calcium is usually present in glasses as a network modifying Ca^{2+} cation although other researchers have observed that, in certain formulations, a significant proportion of the calcium species actually form linkages within the silicate network [5,20]. Calcium linked into the silicate network would be less readily soluble than that in a network modifying role. Hence, despite the higher $CaO:SiO_2$ ratio of sample 30C:70S relative to that of sample 20C:80S, it is suggested that a greater proportion of the calcium species present in the former sample is participating in network formation.

Recent research has shown that dissolved silicate species from bioactive glasses and ceramics operate at a genetic level to influence the osteoblast cycle. Soluble

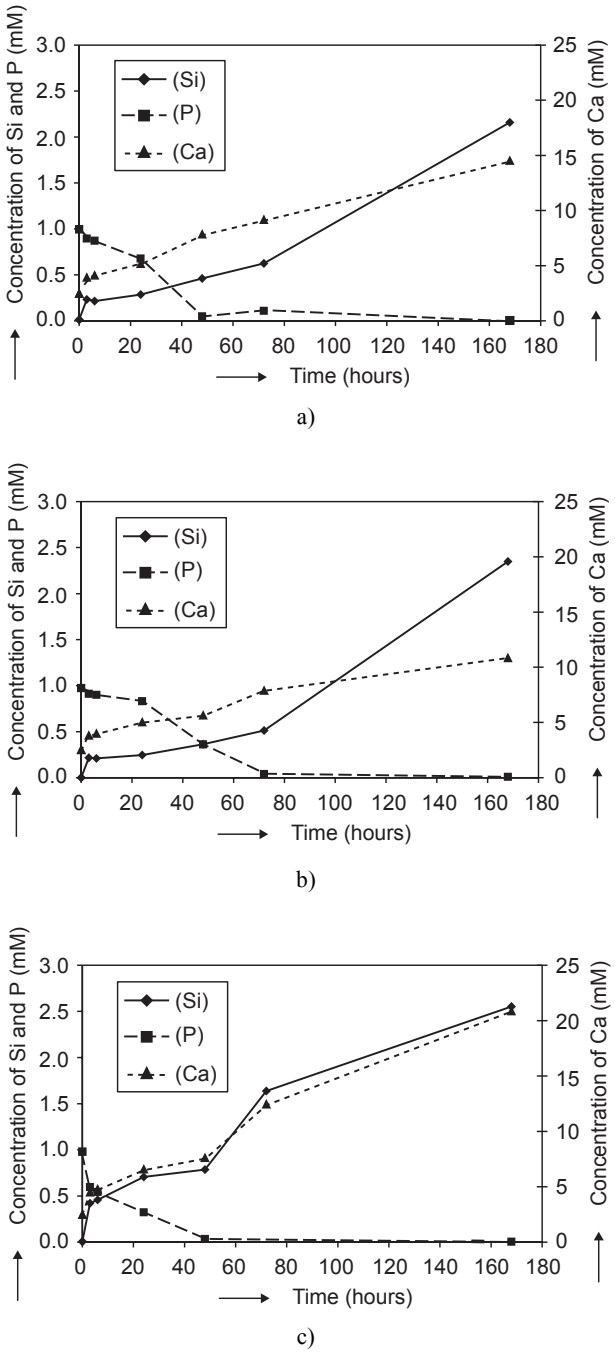

Figure 6. Concentrations of Ca, P and Si in SBF as functions of residence time for a) 20C:80S, b) 30C:70S and c) 40C:60S.

silicate species are now known to enhance the expression of genes and increase the production of growth factors which regulate bone-growth [21,22]. In this respect, it is envisaged that the release of silicates, as shown in Figure 6, will confer additional *in vivo* bioactivity on the binary gel glasses.

Changes in specific surface area and pore volume of the gel-derived glasses as functions of residence time in SBF are plotted in Figures 7 and 8, respectively. In each case, the error bars represent one standard deviation of the mean value plotted on the ordinate axis. Progressive decreases in specific pore volume during the first 72 hours correspond with the deposition of the HA-layer in the mesopore structures and subsequent increases arising from the continued dissolution of the glass matrices are seen after this time (Figure 8). Similar trends in specific surface area are observed for samples 20C:80S and 30C:70S (Figure 7); however a steady increase in surface area as a function of residence time is noted for 40C:60S indicating persistent net dissolution of the surface during the HA precipitation process. This sustained dissolution may account for the poor crystallinity of the HA-layer formed on the surface of this sample.

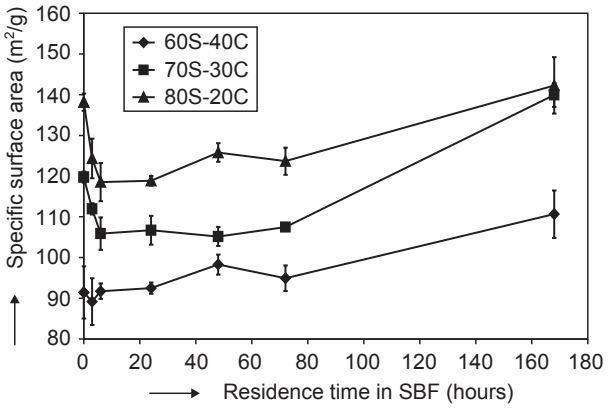

Figure 7. Changes in specific surface area of binary gel-derived glasses as functions of residence time in SBF.

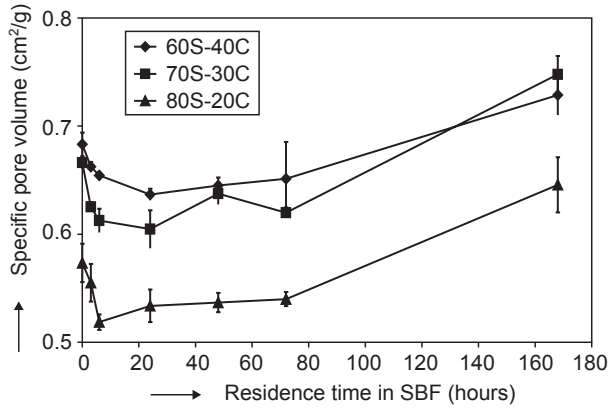

Figure 8. Changes in specific pore volume of binary gel-derived glasses as functions of residence time in SBF.

CONCLUSION

The textural properties of gel-derived two-component $CaO–SiO_2$ glasses have been shown to vary with composition. Pore diameter, specific pore volume, skeletal density and porosity all increased with increasing CaO-content, but specific surface area decreased. The glasses were shown to have free silanol groups on their surfaces and to consist, predominantly, of Q^4 and Q^3 silicate units. The silicate network of the 0.2 CaO mole fraction glass was highly polymerized, but with increasing CaO mole fraction, depolymerisation led to the occurrence of isolated SiO_4 tetrahedra within the glass matrix. Unusually, even at higher mole fractions of CaO, these glasses retained a proportion of Q^4 and Q^3 species.

All glass formulations were bioactive, as determined by precipitation of hydroxyapatite on exposure to SBF; however, rate of formation of apatite did not vary linearly with composition, but increased in the order 0.2 CaO > 0.4 CaO > 0.3 CaO. This differential bioactivity was attributed to the rates of dissolution of calcium from the glass matrices and variations in the proportion of Ca^{2+} participating in network formation.

References

1. Kokubo T.: Materials Science and Engineering C *52*, 97 (2005).
2. Kokubo T., Takadama H.: Biomaterials *27*, 2907 (2006).
3. Fujita Y., Yamamuro T., Nakamura T., Kotani S.: J.Biomed.Mater.Res. *25*, 991 (1991).
4. Kotani S., Fujita Y., Kitsugi T., Nakamura T., Yamamuro T.: J.Biomed.Mater.Res. *25*, 1303 (1991).
5. Lockyer M.W.G., Holland D., Dupree R.: J.Non-Cryst. Solids *188*, 207 (1995).
6. Peltola T., Jokinen M., Rahiala H., Levänen E., Rosenholm J. B., Kangasniemi I., Yli-Urpo A.: J. Biomed. Mater.Res. *44*, 12 (1999).
7. Martínez A., Izquierdo-Barba I., Vallet-Regí M.: Chem. Mater. *12*, 3080, (2000).
8. Li P., Othsuki C., Kokubo T., Nakanishi K., Soga N.: J.Am.Ceram.Soc. *75*, 2094 (1992).
9. Vallet-Regí M., Salinas A.J., Martínez A., Izquierdo-Barba I., Pérez-Pariente J.: Solid State Ionics *172*, 441 (2004).
10. Saravanapavan P., Hench L.L., J. Biomed.Mater.Res. *54*, 608 (2000).
11. Coleman N.J., Hench L.L.: Ceram.Int. *26*, 171 (2000).
12. Bellantone M., Coleman N.J., Hench L.L.: J.Biomed. Mater.Res. *52*, 484, 2000.
13. Brunauer S., Deming L.S., Deming W.S., Teller J.: Am.Chem.Soc. *62*, 1723 (1940).

14. Thomas M.A., Coleman N.J.: Colloids and Surfaces A. *187*, 123 (2001).
15. Sing K.S.W., Everett D.H., Haul R.A.W., Moscou L., Rouqurol R.A., Rouqurol J.R., Siemiewska T.: Pure Appl. Chem. *57*, 603 (1985).
16. de Boer J.H., Lippens B.C., Linsen B.G., Broekhoff J.C.P.: J.Colloid Interface Sci. *21*, 405 (1966).
17. Hayashi T., Saito H.: J.Mater.Sci. *15*, 1971 (1980).
18. Mägi M., Lippmaa E., Samoson A., Engelhardt G., Grimmer A.-R.: J.Phys.Chem. *88*, 1518 (1984).
19. Ohtsuki C., Kokubo T., Yamamuro T.: J.Non-Cryst. Solids *143*, 84 (1992).
20. Veal B.W., Lam D.J., Paulika A.P., Ching W.Y.: Non-Cryst.Solids *49*, 309 (1982).
21. Xynos I.D., Edgar A.J., Buttery L.D.K., Hench L.L., Polak J.M.: J.Biomed.Mater.Res. *155*, 151 (2000).
22. Patel N., Best S.M., Bonfield W., Gibson I.R., Hing K.A., Damien E.: J.Mater.Sci.Mater.Med. *13*, 1199 (2002).

TEXTURNÍ A STRUKTURNÍ VLASTNOSTI BIOAKTIVNÍCH SKEL V SYSTÉMU $CaO–SiO_2$

NICHOLA J. COLEMAN, MARIA BELLANTONE*, JOHN W. NICHOLSON, ANDREW P. MENDHAM

School of Science, University of Greenwich, Chatham Maritime, Kent, ME4 4TB, UK
**Nature Materials, The Macmillan Building, 4 Crinan Street, London, N1 9XY, UK*

Byla připravena a pozorována binární skla CaO odvozená od gelu $CaO–SiO_2$ s molárními podíly 0,2, 0,3 a 0,4. Zjistilo se, že průměr pórů, specifický objem pórů, skeletová hustota a poréznost narůstají s rostoucím obsahem CaO, zatímco dochází k doprovodnému jevu zmenšování specifického povrchu. Měření ^{29}Si NMR ukázalo, že 0,2 molární frakce CaO skla se skládala z vysoce polymerizovaných silikátových druhů Q^4 a Q^3 s několika jednotkami Q^2. Se zvyšující se molovou frakcí CaO se tyto silikátové druhy rychle depolymerizovaly, takže ve skelné matrici 0,4 CaO byly zjištěny izolované tetrahedra SiO_4. Při narůstající molárním podílu CaO sklo překvapivě vykázalo obsah druhů Q^4 a Q^3. Všechna skla o různém složení jevila bio-aktivitu in vitro. Rychlost srážení hydroxyketonů sledovala pořadí 0,2 CaO > 0,4 CaO > 0,3 CaO, což je efekt způsobený rozdílem v rychlosti rozpouštění vápníku v těchto sklech. To se naopak zdá být závislé na množství Ca^{2+} zastoupeného ve skelné síti.